Eur Biophys J (2012) 41:249–256
DOI 10.1007/s00249-011-0782-4

ORIGINAL PAPER

EBSA
Biophysics in Europe

Towards the realization of label-free biosensors through impedance spectroscopy integrated with IDES technology

R. Di Capua · M. Barra · F. Santoro · D. Viggiano · P. Ambrosino · M. V. Soldovieri · M. Tagliatela · A. Cassinese

Received: 15 May 2011 / Revised: 8 December 2011 / Accepted: 12 December 2011 / Published online: 12 January 2012

Abstract Impedance spectroscopy (IS) is a powerful technique for analysis of the complex electrical impedance of a large variety of biological systems, because it is sensitive both to surface phenomena and to changes of bulk properties. A simple and convenient method of analysis of cell properties by IS is described. An interdigitated electrodes configuration was used for the measurements; human epithelial cells were grown on the device to investigate the complex dielectric response as a function of frequency, in order to test the suitability of the device for use as a label-free biosensor. To test the ability of the device to detect channels in the cell membrane, the effect of drugs known to affect membrane integrity was also investigated. The frequency response of the admittance (i.e. the reciprocal of the impedance) can be well fitted by a model based on very simple assumptions about the cells coating the device surface and the current flow; from the calculations, membrane-specific capacitance and information about cell adhesion can be inferred. These preliminary efforts have shown that our configuration could lead to a label-free non-invasive technique for biosensing and cellular behavior monitoring which might prove useful in investigation of the basic properties of cells and the effect of drugs by estimation of some fundamental properties and modification of the electrical characteristics of the device.

R. Di Capua (✉) · D. Viggiano · P. Ambrosino · M. V. Soldovieri · M. Tagliatela
Health Sciences Department, University of Molise, Campobasso, Italy
e-mail: roberto.dicapua@unimol.it

R. Di Capua · M. Barra · F. Santoro · A. Cassinese
CNR-SPIN and Department of Physical Science, University of Naples Federico II, Naples, Italy

Keywords Impedance spectroscopy · Impedance analysis · Sensors · Interdigitated electrodes · Cell membrane integrity

Introduction

In the last decade, interest in dielectric spectroscopy or impedance spectroscopy (IS) as a means of probing biological material has increased substantially because of its versatility and relative technical simplicity. In particular, IS is a non-invasive and label-free technique, proved to be a suitable for characterization of biological material, and monitoring the state of individual cells, or some features of tissues, without affecting survival. For this reason, use of IS for such applications has been investigated and improved for many years, and it has recently been used to study membrane potential (Bot and Prodan 2009), to monitor the cellular modifications consequent of substrate adhesion during apoptosis (Arndt et al. 2004) and cell growth (Cho and Thielecke 2008), to measure the passive electrical properties of cells on substrates (Ceriotti et al. 2007a, b), and for several specific applications as described by Lisdat and Schäfer (2008). One of the most intriguing applications of IS is for biosensing purposes (Lisdat and Schäfer 2008; Katz and Willner 2003), which exploits the effective relationship between the physical principles of IS and biological and physiological concepts. IS-based biosensor prototypes have been produced, for example, for nucleic acid detection (Strasak et al. 2002; Park et al. 2005; Kafka et al. 2008), immunosensing (Hleli et al. 2006; Pan 2007), detection of enzymes, viruses, and bacteria (Dickert et al. 2003; Cortina et al. 2006; Yang and Li 2006; Maalouf et al. 2007), and to measure the response of embryos to cryoprotectant (Wang et al. 2006, 2007).

With regard to cell properties and behavior, IS has been used to study cellular micro-movements, cell adhesion, proliferation and cytotoxicity, intercellular resistance, DNA content, cell volume/shape, receptor stimulation, and charge transport across membranes and membrane/solution interfaces (Bot and Prodan 2009).

In this context, the objective of this work was to implement a prototypical chip-based system for monitoring the impedance versus frequency behavior of a cell layer attached to a substrate in a culture medium. The choice of geometrical and electrical configuration was driven by consideration of already characterized devices and possible future developments. The methodology proposed here combines three features:

1. it uses a silicon substrate, which enables further electrical control and application of electrical stimuli to test the electrochemical properties of the cell membrane;
2. the device implements interdigitated gold electrodes coupled with a small volume of culture medium to achieve optimum sensitivity toward cellular properties; and
3. control electrodes without cells are exposed to the same medium as the cells, thus controlling in real time for the effects on the culture media of the chemical compounds tested.

The performance of such a device as a biosensor for detection of cells and for investigation of their response to stimuli has been tested by operating on a cell layer grown on the chip. The frequency dependence of the complex impedance has been measured and analyzed, and the variation of the signal with time as a consequence of addition of Nystatin and Triton X-100 is reported.

Materials and methods

HeLa cells culture and fluorescence microscopy

For the experiments, human epithelial (HeLa) cells, derived from human cervical cancer cells, were used. The advantage of this immortalized cell line, which is widely used in biological research, is the short replication time and the resistance to environmental perturbations. Moreover, HeLa cells form stable, homogeneous cellular monolayers, with good adhesion between cells, an important feature for this experimental set up.

HeLa cells were grown in RPMI 1,640 with L-glutamine and 10% foetal calf serum (FBS) plus 50 units/ml penicillin and 50 g/ml streptomycin in a humidified 5% CO_2 atmosphere at 37°C. Cells were then seeded into 24-well plates (2×10^6 cells per well) containing the Si^{++}/SiO_2/Au substrates (described below), which had previously been mechanically cleaned under water and ethanol, paying attention to avoid damage to gold electrodes, and sterilized by use of UV light for at least 30 min; this procedure enabled reuse of the same substrates up to ten times.

Visual inspection of the substrate using a high magnification lens with monochrome camera and epiillumination showed that the cellular monolayer was intact before the measurements. Moreover, to assess cell morphology, before and after the measurements, random substrates were fixed in ethanol 70% and then stained with Hoechst 33,258 and propidium iodide (PI) for 5 min to visualize cell nuclei and cell shape, respectively (Fig. 1). After fixation, PI can enter all cells, visualizing double-stranded DNA (in the nucleus) and RNA (in the cytoplasm), thereby giving a strong fluorescent signal for the cell contours.

After washing with PBS, stained cells were identified under a fluorescence microscope (Leica DMI3000) by using excitation/emission wavelengths of 340/440 and 568/585 nm for Hoechst 33,258 and PI, respectively. These fluorescent markers were selected because of their strong fluorescence emission and their minimum crosstalk with the possible fluorescence signal emitted by the substrate.

Structure of interdigitated electrodes

The impedance versus frequency measurements were performed by use of interdigitated electrode system (IDES) consisting of a heavily n-doped silicon (S^{++}) substrate, a 200 nm thick silicon dioxide (SiO_2) thermally grown layer, and interdigitated gold electrodes. This geometry is also a basis for a field-effect transistor (FET) structure: the gold microelectrodes in a pair of adjacent devices act as the source–drain contacts (Fig. 2), the gate contact being the Si^{++} substrate itself. Although in this experiment we did not exploit its full potential, there are several reasons to use an FET device with an IDES structure. Among the advantages of an FET for cell characterization, the high sensitivity to the changes in electrical signals and capacitances or ion process and the ease of integration into larger signal-processing systems are the most obvious (Lehmann et al. 2000, 2001; Poghossian et al. 2009); from the perspective of basic characterization for biosensing purposes, it will enable the introduction in future experiments of further external stimuli of an electrical nature, for example application of a dc electrical field, possibly affecting the cellular growth. In addition, it is suitable for integration of the traditional technology based on inorganic semiconductors with the use of organic semiconductors as active channels; this should guarantee greater compatibility with biological material in non-invasive studies, which is a fundamental requirement for further cellular application. In this work, we performed our tests with cells directly lying on the SiO_2 substrate. With regard to the in-plane IDES

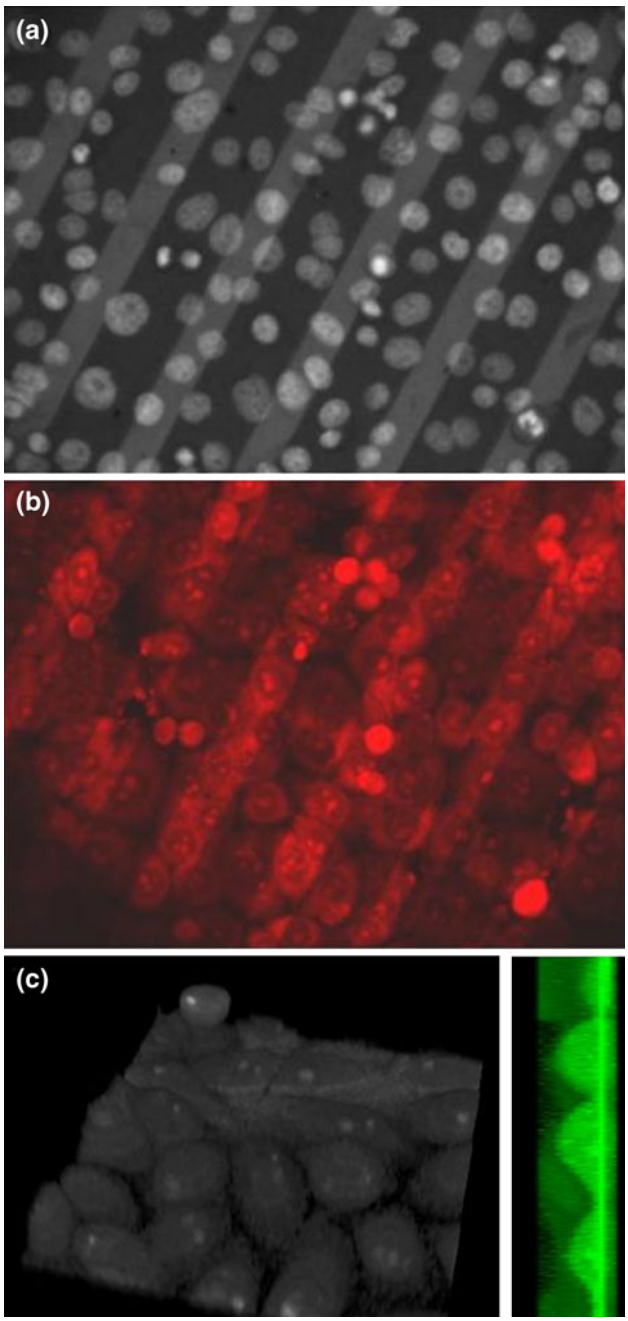

Fig. 1 **a** Cell nuclei and **b** cell shape visualized by staining with Hoechst 33,258 and PI, respectively; **c** 3D reconstruction from serial optical sections of HeLa cells coating the device; on the right a lateral projection of the cell layer is shown to emphasize the thickness of the organic material (*scale bar* 10 μm)

geometry, at variance with conventional designs, the current flow occurs very close to the surface, resulting, therefore, in much greater sensitivity to any changes in cell culture properties. Furthermore, realization of the complete electrode configuration on the same chip improves the possibility of integration in external circuits, because no external electrodes are needed (Ehret et al. 1997; Lisdat and Schäfer 2008).

Experimental conditions

The devices were physically connected to an impedence-measurement system (Fig. 2), an Agilent 4,284 LCR meter, which applied an AC signal with amplitude of 100 mV. IS spectra were recorded at room temperature (approx. 22°C). After plating, the cells were mechanically removed from one of the two gold electrode arrays, to obtain, on the same chip, one electrode array covered by cells, and another devoid of cells (Fig. 2). This configuration enabled exposure of the whole chip to the different experimental conditions and use of the cell-free array as an internal control, thus enabling discrimination of the cellular contribution to the measured variations induced by external stimuli. This configuration also enabled better control over possible fluctuations of the impedance spectra as a result of time drift or chemicals added to the media. Throughout the experiments, cells were incubated in the presence of a fixed volume (50 μl) of normal Krebs (NK), a volume which resulted in optimum device sensitivity.

Results and discussion

The LCR meter provides the complex admittance $Y = Z^{-1}$, where Z is the complex impedance of the connected load circuit. Y can be expressed either by real and imaginary parts or by modulus and argument; in Fig. 3a–d all these physical quantities are plotted as a function of the frequency in the range 100 Hz–100 kHz recorded from both cell-covered and cell-free electrodes. Note that at the lower frequency the effect of the presence of cells does not affect the values measured, which were, in contrast, substantially modified in the range 10–100 kHz; this seems to be a common feature in experiments performed in similar planar configurations (Giaever et al. 1991; Arndt et al. 2004; Cho et al. 2008), probably because of the presence of the phospholipid bilayer of the cell membrane which creates a sort of ion separation between the extracellular and intracellular environments (Giaever et al. 1991; Prodan et al. 2008). It is important to note that the presence of cell-free electrodes in the same solution of the cell-covered electrodes is the optimum situation for controlling shifts in the impedance spectra because of temperature, pH, or chemicals released in the medium. Previous experiments, in fact, used detergents to detach cells at the end of the experimental session (Ceriotti et al. 2007a) or used control electrodes in solutions physically separated from the cell solution.

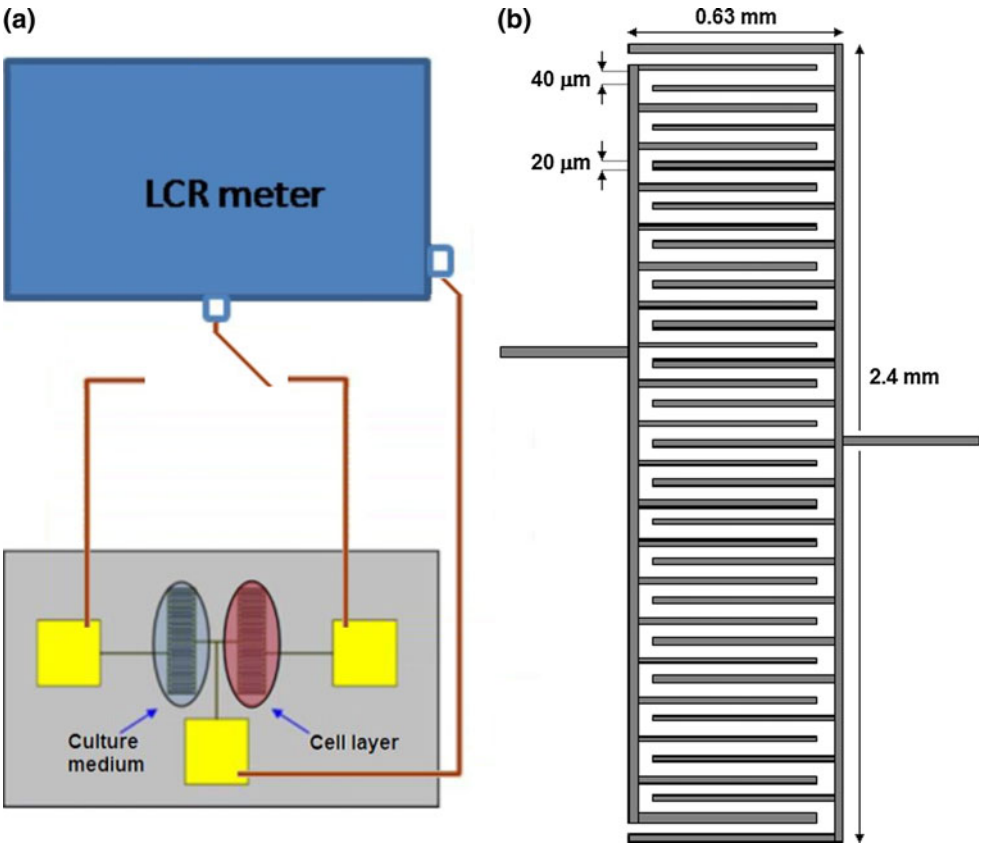

Fig. 2 **a** IDES structure with the gold electrodes, and the possibility of switching the measurement from the cell layer to the empty culture medium. **b** Schematic diagram of the design of the electrodes, showing the width of the gold lines, the spacing between them, and the whole structure

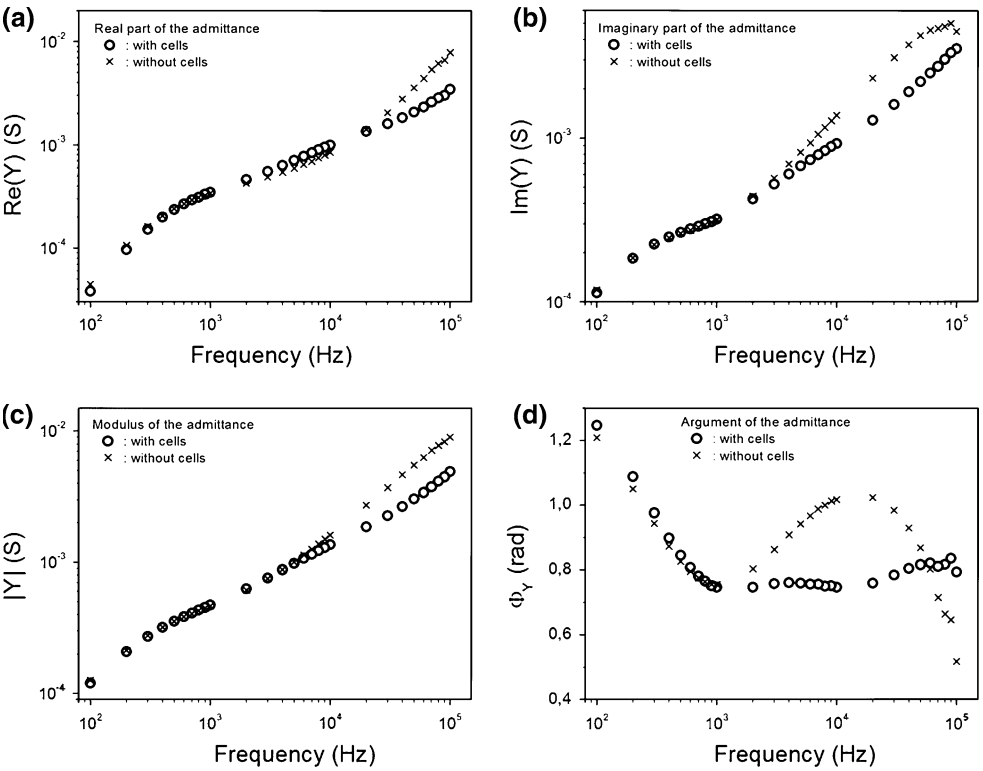

Fig. 3 **a** Real and **b** imaginary parts, **c** modulus and **d** argument, of the complex admittance plotted as a function of frequency for solution with and without cells. The exciting voltage had an amplitude of 100 mV at all frequencies

To test the capability of the device to detect the effects of external stimuli, we monitored the complex admittance as a function of time while adding drugs known to affect membrane integrity, for example Nystatin and Triton X-100; in these experiments, the frequency of the electrical signal was fixed at 30 kHz, a value at which the difference between the responses from channels without and with cells was maximum (Fig. 3). Nystatin is a polyene antibiotic which forms channels in the cell membrane bilayer that are selective to monovalent ions or uncharged molecules smaller than approximately 0.8 nm, maintaining the cells viable and attached to the substrate; a sudden decrease of both real and imaginary parts of the admittance is actually observed when Nystatin (120–240 μg/ml) is dropped in the solution, demonstrating that this range of impedance was sensitive to the electrical properties of the cell membrane. Triton X-100 (0.2% in NK solution), in contrast, physically dissolves the cell membrane, enabling the intracellular and extracellular liquids to merge; as a consequence the admittance of the solution is similar to that recorded by the channel with the culture medium alone. Plots showing these effects are reported in Fig. 4. The effects of Nystatin resemble those reported by Malleo et al. (2009), who interpreted the effects of adding streptolysin (which, similar to Nystatin, creates pores) as an osmotic change in the cell size; the observed effect of Triton X-100 is in reasonable agreement with that reported by Rümenapp et al. (2009), who reported that Triton made the impedance of the cell solution similar to that of the free medium in the high-frequency range. The fact that, in the time domain also, impedance changes were also observed in the electrodes without the cell layer, is a strong indication of the need to monitor cell-free device behavior to properly distinguish the electrical responses from those related to the effects of the added substances on the cells.

Whereas response versus time as a consequence of external stimuli an has immediate qualitative and quantitative interpretation, the frequency dependence of the dielectric properties must be correctly interpreted to infer some basic properties of the biological material under investigation. Different theoretical models have been proposed, on the basis of several microscopic or phenomenological arguments. These include general considerations on electrochemical dielectric spectroscopy, properties of cell suspensions, features of current flows in cell layers, dispersion mechanisms, and dielectric relaxation because of interfacial polarization (Giaever et al. 1991; Grosse and Schwan 1992; McAdams et al. 1995; Zhang et al. 1995; Mihai et al. 1996; Asami 2002, 2006; Morgan et al. 2007; Prodan et al. 2008; Bot and Prodan 2009).

In our experiment the electrodes were placed on the bottom of the liquid drop, both in the solution with the cells and in the cell-free medium, rather than being enclosed in the liquid mixture; the cells were then covering them instead to being suspended in the solution. The current flow and impedance versus frequency function for this electrodes and cells configuration is well described by the model first developed by Grosse and Schwan (1992), and recently used for quantitative measurements in similar experimental configurations (Arndt et al. 2004; Morgan et al. 2007). In particular, this model has been applied by Morgan et al. (2007) to the results of an IS experiment conducted with the electrodes in an IDES geometry similar to that used here.

The basic assumptions of the model refer to the shape of the cells, regarded as circular disks, and to the path of the current, assumed to flow in the space between the lower part of the cells and the substratum. Both assumptions are quite reasonable, considering the distribution of the cells in Fig. 1: the cells appear to be disk-like in shape, and do not overlap each other, so no "spurious" (from the perspective of the model assumptions) current lines are created.

Under such conditions the following relationship can be written:

$$\frac{Y_c(f)}{Y_n(f)} = \left(\frac{j\pi f C_m}{Y_n(f) + j\pi f C_m} + \frac{\frac{Y_n(f)}{Y_n(f)+j\pi f C_m}}{\frac{j\gamma r_c}{2}\frac{I_0(\gamma r_c)}{I_1(\gamma r_c)} + \frac{2}{G_b}(Y_n(f) + j\pi f C_m)} \right)$$

where $Y_n(f)$ represents the complex specific admittance (the reciprocal of the impedance), i.e. per surface unit, of

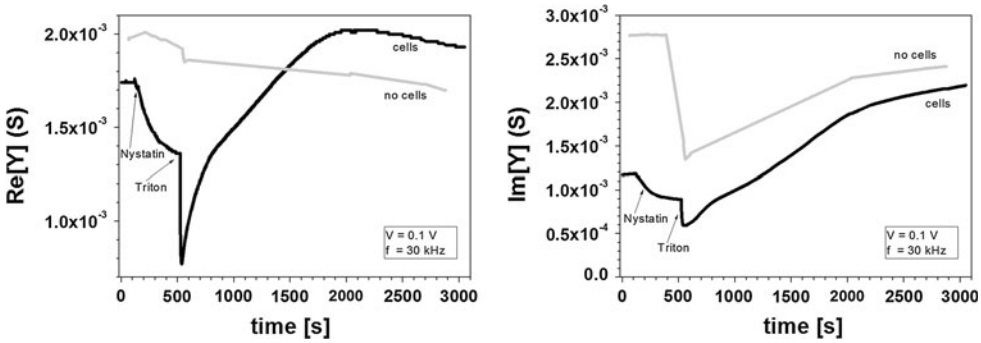

Fig. 4 Real and imaginary parts of the admittance plotted as a function of time when Nystatin (first) and Triton X-100 (later) are dropped into the solution

the cell-free electrodes as a function of the frequency f, and $Y_c(f)$ is the same quantity for the electrodes coated with the cell layer. In our experiment we measured the total (non-specific) admittance for both media; because of the geometrical equivalence of the couple of electrodes in the two situations, the ratio is not affected by the surface normalization, and the left side in the previous equation can be regarded as a directly measured quantity. However, in the right side Y_n is not scaled by Y_c, so estimation of the area of the electrodes is needed for this part; the chip surface extensions are approximately 10^{-1} cm^2. C_m is the specific membrane capacitance and G_b the specific conductance between adjacent cells, and here are considered as fitted terms. I_0 and I_1 are zero and first-order modified Bessel functions of the first kind, j represents the imaginary unit and γr_c is defined as:

$$\gamma\, r_c = r_c\sqrt{\frac{\rho}{h}\left(Y_n(f) + j\pi f\, C_m\right)} = \alpha\sqrt{\left(Y_n(f) + j\pi f\, C_m\right)}$$

where r_c is the average cell radius, ρ the resistivity of the solution, and h the separation between the cells and the substratum; $\alpha = r_c(\rho/h)^{1/2}$ is another fitted term. Because r_c and ρ are easily measurable quantities, h could be inferred from the best value of α. This is, however, beyond the experimental purpose of this work, because the main objective is the testing of our prototypical biosensor, and we regarded α as merely a variable in the least squares procedure. Note that, because of its definition, γ, also, is frequency-dependent.

The results of the fit are shown in Fig. 5 for both the imaginary and real parts of Y_c. The best-fit curves are obtained with $C_m = 10$ μF/cm^2, $\alpha = 5\ \Omega^{-1/2}$ cm, and $G_b = 10^{-2}\ \Omega^{-1}$ cm^{-2}. The specific membrane capacitance thus derived is higher than the nominal specific capacitance assumed for the same cell type (e.g. 1.9 μF/cm^2 for HeLa cells, Asami et al. 1990). By assimilating the cell as a double disk with a diameter of approximately 10 μm, as directly measured by the microscope, a membrane capacitance of approximately 50 pF is calculated; this value is larger than that obtained by the patch clamp technique on the same cells. The larger specific membrane capacitance calculated by impedance spectroscopy might reflect the presence of additional lipidic membranes below the cell membrane (e.g. the nuclear envelope and the endoplasmic reticulum). The cell radius is also included in the definition of α; by assuming the medium resistivity $\rho = 0.2\ \Omega$ m, the best fit value for α leads to $h \approx 10$ nm. Because $h \ll r_c$, we can reasonably assert that the cells actually form a layer coating the electrodes rather than a suspension in solution. By characterizing several biological systems, the relative values of h and G_b obtained by this procedure can provide information about cell adhesion and about the reciprocal electrical interaction.

Conclusions

The application of IDES technology to IS characterization of cell layers leads to the possibility of realization of an innovative device in the field of biosensors. The interdigitated geometry with the FET architecture ensures high electrical sensitivity and good flexibility for testing the responses of the biological samples under study. In this work, we demonstrated that it is possible to correctly place and grow an intact cell monolayer, as confirmed by the optical and fluorescence microscopy observations. Our data on the admittance showed the effective working of the device as a biosensor. Theoretical analysis of the frequency dependence of the admittance revealed that the mechanisms of current flow in the cell layer placed on the IDES electrodes follows a simple model based on the role of basic cell features and on their adhesion to the substrate. The effect of addition of Nystatin and Triton X-100 proved the sensitivity in measuring the responses of the cell membrane to external stimuli, with a fast and large response: the response to Nystatin shows that the system is sensitive to the electrical properties of the membrane, and the reaction to Triton X-100 indicates the signal effectively depends on cell membrane adhesion to the electrodes. Such

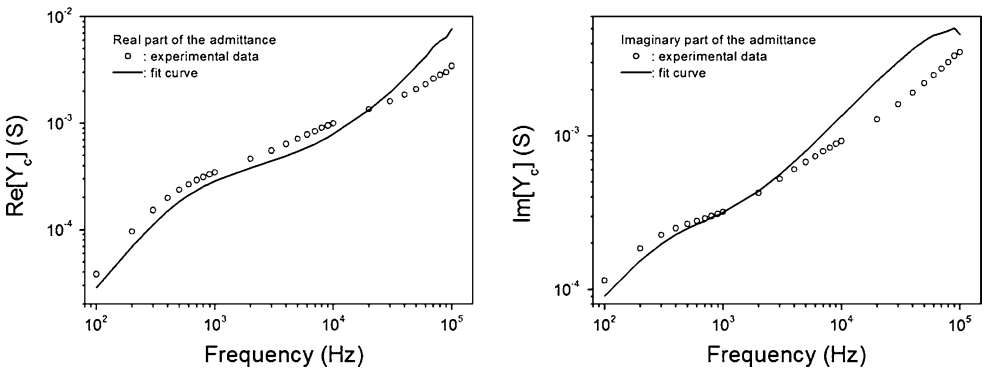

Fig. 5 Frequency dependence of the real and imaginary parts of the admittance fitted by the model described in the text

observations demonstrate the capability of our system to detect the behavior of the cell membrane; by modifying the layout details it will be possible to improve the sensitivity and to record the membrane potential.

Several aspects of further progress are still to be investigated. Qualitative consideration of variation of the effects with time after addition of drugs can be supported by a more quantitative evaluation procedure. Quantitative modeling of frequency dependence could give important information about cell features if coupled with further characterization for determining fitting data. Further experimental improvement will be achieved by applying gate signals to the chip, enabling investigation of active (voltage-dependent) and passive (capacitive) properties of the cells.

Acknowledgments This work was partially supported by a grant from the Department of Health Sciences, University of Molise. Financial support from the regional projects MEDIREN "Innovative methods and devices for the detection of electrophysiology parameters from neuronal cells and tissues" is gratefully acknowledged.

References

Arndt S, Seebach J, Psathaki K, Galla HJ, Wegener J (2004) Bioelectrical impedance assay to monitor changes in cell shape during apoptosis. Biosens Bioelectron 19:583–594

Asami K (2002) Characterization of heterogeneous systems by dielectric spectroscopy. Prog Polym Sci 27:1617–1659

Asami K (2006) Dielectric dispersion in biological cells of complex geometry simulated by the three-dimensional finite difference method. J Phys D Appl Phys 39:492–499

Asami K, Takahashi Y, Takashima S (1990) Frequency domain analysis of membrane capacitance of cultured cells (HeLa and myeloma) using the micropipette technique. Biophys J 58: 143–148

Bot C, Prodan C (2009) Probing the membrane potential of living cells by dielectric spectroscopy. Eur Biophys J 38:1049–1059

Ceriotti L, Ponti J, Broggi F, Kob A, Drechsler S, Thedinga E, Colpo P, Sabbioni E, Ehret R, Rossi F (2007a) Real-time assessment of cytotoxicity by impedance measurement on a 96-well plate. Sens Actuators B 123:769–778

Ceriotti L, Ponti J, Colpo P, Sabbioni E, Rossi F (2007b) Assessment of cytotoxicity by impedance spectroscopy. Biosens Bioelectron 22:3057–3063

Cho S, Thielecke H (2008) Electrical characterization of human mesenchymal stem cell growth on microelectrode. Microelectron Eng 85:1272–1274

Cortina M, Esplandiu MJ, Alegret S, del Valle M (2006) Urea impedimetric biosensor based on polymer degradation onto interdigitated electrodes. Sens Actuators B 118:84–89

Dickert FL, Hayden O, Lieberzeit PA, Haderspoeck C, Bindeus R, Palfinger C, Wirl B (2003) Nano-and micro-structuring of sensor materials—from molecule to cell detection. Synth Met 138: 65–69

Ehret R, Baumann W, Brischwein M, Schwinde A, Stegbauer K, Wolf B (1997) Monitoring of cellular behaviour by impedance measurements on interdigitated electrode structures. Biosens Bioelectron 12:29–41

Giaever I, Keese CR (1991) Micro motion of mammalian cells measured electrically. Proc Natl Acad Sci USA 88:7896–7900

Grosse C, Schwan HP (1992) Cellular membrane potentials induced by alternating fields. Biophys J 63:1632–1642

Hleli S, Martelet C, Abdelghani A, Burais N, Jaffrezic-Renault N (2006) Atrazine analysis using an impedimetric immunosensor based on mixed biotinylated self-assembled monolayer. Sens Actuators B 113:711–717

Kafka J, Pänke O, Abendroth B, Lisdat F (2008) A label-free DNA sensor based on impedance spectroscopy. Electrochim. Acta 53:7467–7474

Katz E, Willner I (2003) Probing biomolecular interactions at conductive and semiconductive surfaces by impedance spectroscopy: routes to impedimetric immunosensors, DNA-sensors, and enzyme biosensors. Electroanalysis 15:913–947

Lehmann M, Baumann W, Brischwein M, Ehret R, Kraus M, Schwinde A, Bitzenhofer M, Freund I, Wolf B (2000) Noninvasive measurement of cell membrane associated proton gradients by ion-sensitive field effect transistor arrays for micro physiological and bioelectronical applications. Biosens Bioelectron 15:117–124

Lehmann M, Baumann W, Brischwein M, Gahle HJ, Freund I, Ehret R, Drechsler S, Palzer H, Kleintges M, Sieben U, Wolf B (2001) Simultaneous measurement of cellular respiration and acidification with a single CMOS ISFET. Biosens Bioelectron 16:195–203

Lisdat F, Schäfer D (2008) The use of electrochemical impedance spectroscopy for biosensing. Anal Bioanal Chem 391:1555–1567

Maalouf R, Fournier-Wirth C, Coste J, Chebib H, Saikali Y, Vittori O, Errachid A, Cloarec JP, Martelet C, Jaffrezic-Renault N (2007) Label-free detection of bacteria by electrochemical impedance spectroscopy: comparison to surface plasmon resonance. Anal Chem 79:4879–4886

Malleo D, Nevill JT, Lee LP, Morgan H (2009) Continous differential impedance spectroscopy of single cells. Microfluid Nanofluidics 9:191–198

McAdams ET, Lackermeier A, McLaughlin JA, Macken D (1995) The linear and non-linear electrical properties of the electrode-electrolyte interface. Biosens Bioelectron 10:67–74

Mihai CM, Mehedintu M, Gheorghiu E (1996) The derivation of cellular properties from dielectric spectroscopy data. Bioelectrochem Bioenerg 40:187–192

Morgan H, Sun T, Holmes D, Gawad S, Green NG (2007) Single cell dielectric spectroscopy. J Phys D Appl Phys 40:61–70

Pan J (2007) Direct and rapid monitoring the biochemical reaction of interleukin-6 in human using a flow-injection capacitive immunosensor in clinical immunoassay. Sens. Actuators B 125:517–525

Park JW, Jung HS, Lee HY, Kawai T (2005) Electrical recognition of label-free oligonucleotides upon streptavidin-modified electrode surfaces. Biotechnol Bioprocess Eng 10:505–509

Poghossian A, Ingebrandt S, Offenhausser A, Schoning MJ (2009) Field-effect devices for detecting cellular signals. Semin Cell Dev Biol 20:41–48

Prodan E, Prodan C, Miller JH Jr (2008) The dielectric response of spherical live cells in suspension: an analytic solution. Biophys J 95:4174–4182

Rümenapp C, Remm M, Wolf B, Gleich B (2009) Improved method for impedance measurements of mammalian cells. Biosens Bioelectron 24:2915–2919

Strasak L, Dvorak J, Hason S, Vetterl V (2002) Electrochemical impedance spectroscopy of polynucleotide adsorption. Bioelectrochemistry 56:37–41

Wang R, Zhang T, Bao QY, Rawson DM (2006) Study on fish embryo responses to the treatment of cryoprotective chemicals using impedance spectroscopy. Eur Biophys J 35:224–230

Wang R, Guan M, Rawson DM, Zhang T (2007) Ultrasound enhanced methanol penetration of zebrafish (Danio rerio) embryos measured by permittivity changes using impedance spectroscopy. Eur Biophys J 37:1039–1044

Yang LJ, Li YB (2006) Detection of viable salmonella using microelectrode-based capacitance measurement coupled with immunomagnetic separation. J Microbiol Methods 64:9–16

Zhang MIN, Repo T, Willison JHM, Sutinen S (1995) Electrical impedance analysis in plant tissues: on the biological meaning of Cole–Cole α in Scots pine needles. Eur Biophys J 24:99–106